I.r. study of solution-grown crystals of polyethylene: correlation with the model from neutron scattering

S. J. Spells, A. Keller and D. M. Sadler
H. H. Wills Physics Laboratory, University of Bristol, Royal Fort, Tyndall Avenue, Bristol BS8 1TL, UK
(Received 28 April 1983; revised 8 September 1983)

The crystal stem arrangement in solution-grown polyethylene crystals has been investigated by the mixed-crystal infra-red technique. Parallel neutron scattering measurements are reported separately. The behaviour of the CD_2 bending vibration is shown to be consistent with a model having 75% adjacent re-entry, 50% dilution of a molecule along the fold plane ({110} direction) and a degree of superfolding equivalent to an average molecular weight ($\bar{M}_w$) of 21 000 for each sheet. This is in agreement with results from neutron scattering, which have previously been interpreted using this model. Computer calculations of stem positions based on these parameters are used to calculate the distributions of doublet splittings for several molecular weights. The main features of low-temperature *FT*i.r. spectra as a function of molecular weight are reproduced in this way.

(Keywords: solution grown; polyethylene; conformation; isotopic labelling; infra-red spectroscopy; adjacent re-entry)

INTRODUCTION

The use of isotopic labelling to identify isolated individual chains has made it possible to study the pathway of an individual polymer molecule in the crystalline state, polyethylene having been used mostly as a well characterized system. Two different methods can be used in this way. Historically the first infra-red spectroscopy, in this application introduced by Krimm and collaborators[2-5] followed several years later by neutron scattering[6-8]. The two methods of investigation were largely pursued independently by the different investigators. However, a combination of the two was necessary for they should both cross-check and complement each other and in combination they should provide more information than each individually. The first attempt to combine the two techniques (the only attempt of this kind to the present day) as applied to solution-grown crystals has been reported previously[8]. Since then further advances have been made by the neutron scattering approach in this laboratory, allowing the specification of the stem arrangement within solution-grown crystals and melt crystallized specimens in greater detail[1]. The present paper is a second stage in the overall approach to invoke the infra-red method and attempt to correlate it with the newly gained knowledge from neutron scattering. For reasons which are explained later, this investigation is confined to solution-grown crystals. First, however, the past history of both the infra-red and the neutron scattering developments needs to be briefly presented.

The general issue relates to the controversial problem of the overall chain trajectory with particular focus on the adjacency or otherwise of the fold re-entry in a given molecule. At the time when the infra-red technique was first applied, the neutron scattering work was at a stage which indicated that the overall shape of a given chain within the crystal was sheet-like with a stem dilution of $\approx 50\%$ and further, that the layer consisted of more than one sheet of stems. The sheet number was shown to increase with molecular weight, an effect attributed to superfolding, i.e. the folding up of individual sheets upon themselves.

BACKGROUND TO INFRA-RED SPECTROSCOPY

Infra-red spectroscopy was the first technique to exploit the potential of using blends of isotopic species. The orthorhombic unit cell of crystalline polyethylene (PE) contains two symmetrically non-equivalent chains giving rise to both in-phase and out-of-phase modes, the frequency difference being the correlation splitting. When deuterated PE (PED) and normal PE (PEH) are crystallized together, bands giving rise to correlation splittings for either species may be monitored. If one species is dilute, then interactions between the guest molecules are minimized and the guest vibrational bands predominantly reflect intramolecular interactions between stems.

The early works of Krimm *et al.* relied on the presence of resolved doublet splittings as evidence of adjacent non-equivalent guest stems and hence of adjacent re-entry along a {110} fold plane[3]. For solution-grown crystals (but not for melt crystallized material which is not considered here further) such a splitting was invariably reported in both isotopic components irrespective of dilution, and the magnitude of the splitting was found to agree with calculated values for highly extended {110} fold planes.

0032-3861/84/060749-10$03.00

It was with this knowledge that a programme of infra-red analysis utilizing labelled guest molecules was initiated. The aim was to provide additional characterization for samples previously investigated by neutron scattering leading to the model quoted. In contrast to previous published work[3] the infra-red measurements were carried out on samples with a wider range of guest molecular weights. Contrary to expectations from previous works a clearly resolved doublet was generally not observed[8]. Only at sufficiently high guest molecular weight and/or concentration was a doublet resolved. The fact that doublets generally did not appear prevented the use of the criterion used in the early works of Krimm to define stem adjacency. Nevertheless the overall width of the band profiles, whether or not the doublet could be resolved, was always greater than for paraffins of identical isotopic composition (and also greater than for bulk material). It was shown to increase with PED molecular weight, indicating a departure from a random arrangement of stems belonging to the same molecule. In a purely empirical manner this excess width was used as a measure of stem adjacency and by comparing with paraffins it was concluded that in single crystals the local concentration of guest stems was in the range of 45–65% for an overall PED concentration of 0.5%. This was at least consistent with the neutron scattering results to the extent that there is a much enhanced local stem concentration as compared to a random stem distribution. Nevertheless, there is some dilution arising from other molecules and both techniques give similar values for its magnitude. No direct evidence of the sheet structure emerged from these i.r. results, but the fact that the observable splitting increases with increasing molecular weight was at least consistent with superfolding: increased interstem interactions were indicated and this is characteristic of a superfolded structure.

After the main work in ref. 8, two important improvements in experimentation became possible which were mentioned, together with their main consequences as a footnote. The first of these was the use of low temperatures which minimizes the variation in lattice dimensions with sample morphology (in this case increasing the splittings) and reduces the i.r. bandwidths. Secondly, a Fourier Transform Interferometer was used, rather than a conventional dispersive spectrometer, to obtain improved signal-to-noise ratios at the low absorption intensities involved. Under only these conditions was band splitting observed as a general feature for all molecular weights. However, this splitting now appeared as a complex multiplet band structure irrespective of whether or not a resolved doublet has been found using the dispersive instrument at room temperature as in the earlier note. This improvement in the spectrum definition allowed the stem dilution to be bracketed within 50–80% with increased confidence (i.e. with a slightly higher mean value than from band-widths alone). The same improvement of the spectrum definition made it possible to revert to the use of the splitting as a general measure of stem interaction as originally claimed in the earlier works[3]. Nevertheless, this is not a straightforward return to the earlier situation of ref. 3. The band shape is complex, requiring special peak separation procedures and a correspondingly more involved interpretation. Thus, the attractively simple solution of ref. 3 is no longer possible. According to this the mere presence of the splitting defined the fold arrangement and, where a splitting was present, a single quantity (the peak separation) defined the stem environment. The more complex band structure, however, is potentially able to yield more information. It is this latter potential which is used in the present paper.

The experimental and theoretical limitations of the earlier i.r. work were in the meantime also recognized by Krimm *et al.*[4], together with the greater complexity of band shape as obtained subsequently at low temperatures. They developed a procedure for interpreting the multiple band structure of the CD_2 bending vibration. The theory of finite chains of coupled oscillators was used to calculate splittings for finite sheets of adjacent stems, and also for multiple sheets such as are implied by the superfolding model.

BACKGROUND TO NEUTRON SCATTERING

The progress made in understanding the chain conformation in solution grown PE, using the neutron scattering technique with similar isotopic mixtures, has recently been reviewed[1]. A brief summary of results and conclusions will suffice here.

The angular dependence of scattered intensity in the intermediate wavevector range indicated that the stems were arranged in sheets[6]. The radius of gyration, obtained at small angles, was remarkably insensitive to molecular weight, providing the first clear evidence of superfolding[7]. Within the intermediate angle region, scattered intensities were typically 50% of predicted values for fully occupied sheets[6,8]. This information, together with evidence of local concentration from i.r. spectroscopy[8] was taken to imply a dilution along the fold plane of $\approx 50\%$ with stems from other molecules. Results from the two techniques (i.e. neutron scattering and i.r.) at this stage were in agreement in as much as they both indicated some molecular dilution, rather than completely regular adjacent re-entry, but the full details of the molecular dilution remained to be determined.

By extending the range of scattering vector to approach the crystallographic region, it was possible to probe the chain conformation on a more local scale[1]. Working within the framework of the results mentioned, computer models have been developed to fit the scattering data. The program simulates the crystallization of a molecule according to statistical parameters and generates 2-dimensional arrays of stem positions for each 'molecule'. A correlation function for the labelled 'molecules' is calculated and, hence, the scattered intensity is computed. Scattering curves derived in this way were compared with experimental curves, corrected for the finite stem radius. As the scattering is predominantly from the crystal stems in these oriented PE mats, the method allows different types of stem arrangement to be tested. Using the figure of 50% molecular dilution, it can be shown that a model with a preference for occupying alternate lattice sites, as suggested by Yoon and Flory[9], should show a peak at twice the nearest neighbour separation. As no peak was observed experimentally, the model was rejected. A random distribution of stems within the folded ribbons was also found to be inadequate, leading to a small-angle intensity lower than that observed, and a wide-angle intensity which was too high. Optimum agreement was obtained for a model with 75% of adjacent stems, using the number of superfolded sheets as the only variable parameter in fitting data for a range of molecular weights. It should be noted that the model is primarily concerned

with the arrangement of the crystal stems, and the scattering gives little direct information on the way in which they are connected. The model parameters are given in *Table 1*, using the additional assumption that the molecule folds along the growth face with the shortest possible folds connecting the stems. In this way, for example, a group of 4 neighbouring stems along the plane of the sheet are assumed to be connected by adjacent folds. Clearly, this assumption provides an upper limit to the proportion of adjacent re-entry consistent with the model of crystal stem positions. *Figure 1* shows a perspective diagram of part of the arrangement of one molecule within a lamella, using folding along the growth face. Regime I crystallization requires that the rate of completion of a single crystal plane is much larger than the rate of nucleation of successive planes (e.g. ref. 10). Competition between molecules for the niche site from which growth occurs could, for example, result in a diluted growth face. It would not, however, provide any mechanism for the superfolding of molecular sheets. For this to occur, a necessary condition appears to be multiple nucleation so that sheets from different molecules can meet on the growth surface.

The models described in *Figure 1* and *Table 1* form the basis for calculations described later.

OBJECTIVES OF THE PRESENT WORK

Typical stem arrangements which have arisen from the latest neutron scattering work are defined and tested to establish whether they are compatible with the complex multiply peaked infra-red bands arising from correlation splitting in the guest molecules.

It should be stressed that the techniques are sensitive to rather different features of molecular conformation. In the case of neutron scattering, the scattered intensity is determined by the spatial arrangement of crystal stems, with correlations on scales ranging from neighbouring lattice site separations to the overall dimensions of a molecule within the lattice. By contrast, the CD_2-bending vibrational splitting in the i.r. spectrum is primarily influenced by nearest neighbour interactions. The two methods, while complementary, provide different types of information.

There are various possible ways to proceed. One is to follow Krimm *et al.*[4] and attempt to fit the band profile to the minimum possible number of doublet components. If the possible stem arrangements are approximated to blocks of multiple sheets with fully adjacent re-entry, then curve-fitting can provide information on representative sizes of such blocks.

Where components of the band profile overlap, ambiguity arises in the possible number of components and their respective splittings. In this case, curve fitting can only provide a limited interpretation in terms of stem arrangements. A procedure which is the inverse of that outlined now becomes necessary: stem arrangement models can be used to calculate i.r. band profiles for comparison with experimental results. Thus, the detailed stem arrangements developed to fit the neutron scattering data can be analysed and used to calculate i.r. spectra. Comparison with experimental i.r. spectra then provides a crucial test for the validity of the molecular models. It is this method which is used through the main part of the paper, to be followed later by the method based on curve fitting, essentially for comparison.

Table 1 Main parameters of models used to calculate infrared spectra

50%	Dilution along fold plane
75%	Probability of adjacent re-entry
7%	Probability of re-entry at sites separated by 1 other stem
5%	Probability of re-entry at sites separated by 2 other stems
10–20	Stems per sheet
21 000	Average molecular weight per sheet

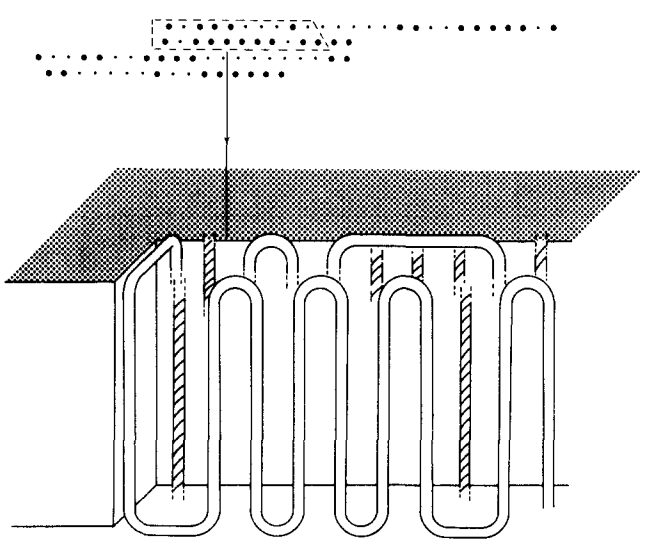

Figure 1 Schematic representation of the molecular conformation of a polyethylene chain within the lamella. The large spots in the crystal stem projection at the top correspond to the unshaded chain the perspective sketch. The {110} direction is horizontal in the projection. The sketch below includes a possible arrangement of the folds

CONFORMATIONAL MODELS

Each set of model parameters is used to generate a series of individual molecular conformations, such as the one shown in *Figure 1*. To clarify the analysis which follows, it is useful to have a 'shorthand' terminology, and this is first described.

Each conformation is initially divided into *groups* of stems, defined as containing stems connected by adjacent {110} folds. To a good approximation, interactions beyond those of nearest neighbours may be neglected in calculating correlation splittings[2], so that each group is effectively independent from the others and the resultant i.r. band profile is the superposition of contributions from each group.

Each group is now transformed into an *equivalent group*. This has a similar number of stems to the original group, and a similar distribution of {110} interactions between stems. The equivalent group has a simpler multiple sheet arrangement of fully adjacent stems, although it may include incomplete sheets. Each sheet starts in register along a {110} plane which is not the fold plane. *Figure 3a* shows an example of an equivalent group, with an incomplete second sheet.

The notation adopted for equivalent group of stems depends on whether all the sheets are complete in having the same number of stems. If this is so, the group is termed *closed*. For a closed group, $(x \times y)$ denotes y sheets, each with x adjacent stems arranged along the fold plane, with the first stem of each sheet in register along a {110} (non-

fold) plane. This is illustrated in *Figure 3b* by an (8 × 3) group, which would have a corresponding doublet splitting of $\Delta\nu_{8\times3}$. A similar structure including incomplete sheets is denoted by $(a, b, c, \ldots)$ where there are a stems in the first, sheet, b stems in the second, c, in the third, etc. The group shown in *Figure 3a* can then be denoted (8, 3), with a splitting $\Delta\nu_{8,3}$. Again, it is implied that the first stem of each sheet is in register.

It is useful to refer to parts of an equivalent group. The (8, 3) group in *Figure 3a*, for example, for example, includes six stems in a double sheet (3 × 2) arrangement. This closed group, forming part of the (8, 3) group, is named a *closed subgroup.*

The molecular conformation of *Figure 2* can be divided into the groups shown. The conformation includes isolated stems, giving rise to no i.r. splittings, and a pair of adjacent stems in the {110} direction, for which the i.r. splitting has been calculated[2]. Two groups of stems form fully adjacent single sheets (C and F) and group E is also effectively a single sheet. However, many stems are within groups of more complex shape (A and D). Cheam and Krimm have used the general theory of coupled oscillators to calculate splittings for finite rows of adjacent stems, both in single and multiple sheets[4]. An arrangement of stems such as those in group D of *Figure 2*, where there is a disruption of simple symmetry by other molecule(s), is no longer amenable to this type of calculation. A complete normal co-ordinate analysis of such a disordered system presents a complex problem, but some progress can be made by a comparison of groups such as D in *Figure 2* with closed groups.

Each group may be characterized by the total number of stems and the numbers of nearest neighbour interactions along {110} planes. Group D, for example, contains a total of 14 stems, 4 with one such interaction, 8 stems with 2, 2 stems with 3 and no stems with 4 interactions. It is now possible to construct an equivalent group with a similar distribution of nearest neighbour interactions. As group D involves no stems with 4 nearest equivalent neighbour interactions, it may be represented by an equivalent double sheet arrangement with one of the sheets uncompleted. The equivalent group then has only one stem with one nearest neighbour interaction. However, the number of stems with 2 and 3 interactions may be fitted to the distribution in group D: solving the simultaneous equations gives 8.5 stems in one sheet and 2.5 in the other. As fractions of stems are not permitted, the numbers must be rounded up or down to the nearest integer. By adjusting them in opposite directions, any error introduced in calculating splittings are minimized. The equivalent group is denoted, therefore, by (8, 3) and corresponds to that shown in *Figure 3a.*

This group has a distribution of nearest neighbour interactions very similar to that of group D in *Figure 2*, the major difference lying in the number of stems with one nearest neighbour interaction. These stems have less influence on the vibrational splitting than stems with multiple interactions: this may be verified by inspecting *Table 2* in ref. 4. The effect of such stems may be neglected to a first approximation. In calculating the i.r. band profiles, the intensity is weighted in proportion to the number of stems in the original group rather than in the equivalent group.

In principle, the splitting for a group of stems involving incomplete sheets may be calculated directly. However, the loss of symmetry compared with a closed group precludes a simple treatment in terms of pairs of interacting oscillators[4]. As an approximation, each stem is considered as an individual oscillator, interacting only with its neighbours in {110} directions. The equations of motion, therefore, involve an interaction force constant and an individual oscillator force constant. The unperturbed oscillator frequency, ν_0, corresponding to an isolated chain stem, is dependent only on the oscillator force constant. Measurement of the minimum frequency of any doublet component (1084.4 cm^{-1} for sample 5 in *Figure 7*), therefore, provides an estimate of the unperturbed frequency. The interaction force constant influences the splitting, calculated independently[4] for an infinite single sheet of stems with adjacent re-entry ($\Delta\nu_{\infty\times1}$): the maximum splitting for a single sheet can be derived from the general solutions to the equations of motion for a free-ended chain of oscillators:[11]

$$\Delta\nu_{\infty\times1} = \sqrt{\nu_0^2 + 4\nu'} - \nu_0$$

where ν_0 is the unperturbed oscillator frequency and ν' is an interaction parameter. Taking $\Delta\nu_{\infty\times1}$ as 5.1 cm^{-1} [4], ν' is calculated as 53.66 cm^{-1}. The equations of motion for a group of stems incorporating incomplete sheets can now be expressed in terms of ν_0 and ν'. The method of solution is straight-forward[11]: periodic solutions are assumed, and the secular determinant is solved for the vibrational

Figure 3 Illustration of the notation used to describe equivalent groups of stems. (a) An (8, 3) group; (b) an (8×3) group

Table 2 Computed doublet splittings for molecular models with 1, 2, 4 and 11 sheets. Brackets correspond to peaks which are not fully resolved

Number of sheets	Equivalent molecular weight	Doublet splittings (cm^{-1})
1	21 000	(2.8), (3.5), 4.6
2	42 000	(2.8), (3.5), 4.6, 7.0
4	84 000	(2.8), (3.5), 4.7, (7.7), 8.4
11	231 000	(2.8), (3.5), 4.6, (6.5), 8.8

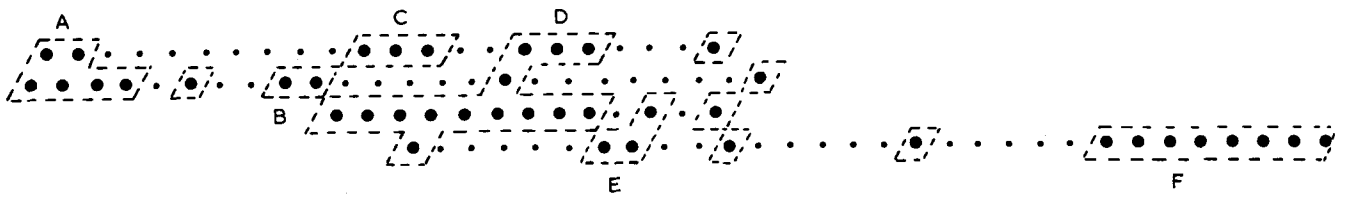

Figure 2 Division of a computer-generated model, shown as a crystal stem projection, into groups of stems which are linked by {110} interactions. As in all diagrams, the {110} direction is horizontal

frequencies. The maximum splitting can then be obtained in terms of ν_0 and ν' and evaluated from the figures quoted. For two simple groups, (3, 2) and (5, 2), this gives splittings $\Delta\nu_{3,2}=5.71\ \text{cm}^{-1}$ and $\Delta\nu_{5,2}=5.84\ \text{cm}^{-1}$.

As this direct calculation of group splittings is unduly cumbersome, approximate methods have been used to reduce computation times. Two methods are discussed here, both involving interpolation from calculated splittings for $(x \times y)$ groups[4]. To demonstrate these, an equivalent group of 2 sheets is considered, denoted by (x, y) with $x \geqslant y$. The first method (a) uses a linear interpolation of the splitting, between the values $\Delta\nu_{x\times1}$ and $\Delta\nu_{x\times2}$:

$$\Delta\nu_{x,y}=\Delta\nu_{x\times1}+\frac{y}{x}(\Delta\nu_{x\times2}-\Delta\nu_{x\times1}) \qquad (1a)$$

The second method (b) uses the closed subgroup $(y \times 2)$ as the basis (with splitting $\Delta\nu_{y\times2}$) with a correction term corresponding to an increase of $(x-y)$ stems in a single sheet group of $2y$ stems:

$$\Delta\nu_{x,y}=\Delta\nu_{y\times2}+(\Delta\nu_{(x+y)\times1}-\Delta\nu_{(2y)\times1}) \qquad (1b)$$

Calculations using both methods are shown in *Figure 4* for the groups (9, 0), (9, 1), . . . , (9, 9), together with splittings for the double sheet sections $(y \times 2)$ plotted against the mean number of interactions per group. Clearly, it is expected that $\Delta\nu_{x,y}\geqslant\Delta\nu_{y\times2}$, since 2 sheets, each with y stems, form part of the (x, y) group. From *Figure 4*, the inequality is not generally satisfied using equation (1a), but it is always satisfied by equation (1b).

The two methods of calculation may be extended simply to numbers of sheets >2. For a group occupying 3 sheets, with x, y and z stems in successive sheets $(x \geqslant y \geqslant z)$, the group is denoted (x, y, z). Method (a) then gives:

$$\Delta\nu_{x,y,z}=\Delta\nu_{x,y}+\frac{z}{y}(\Delta\nu_{y\times2}-\Delta\nu_{y\times1}) \qquad (2a)$$

and for method (b):

$$\Delta\nu_{x,y,z}=\Delta\nu_{z\times3}+(\Delta\nu_{(y+z/2)\times2}-\Delta\nu_{(3z/2)\times2}+(\Delta\nu_{(x+y+z)\times1}-\Delta\nu_{(2y+z)\times1}) \quad \text{for } z\geqslant2 \qquad (2b)$$

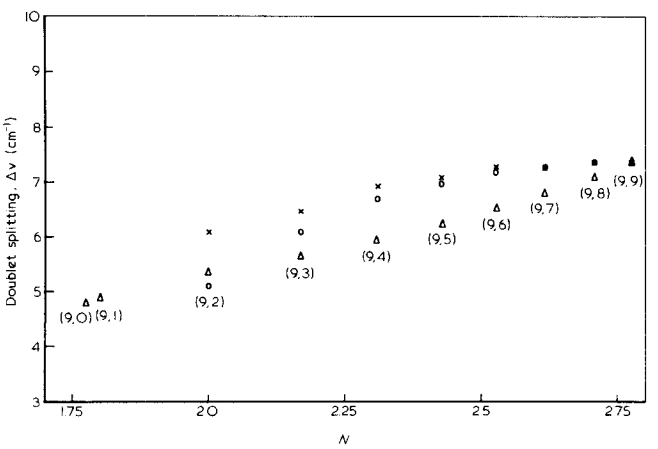

Figure 4 Calculated doublet splittings for (9, y) groups, with $y=0, 1, \ldots, 9$, plotted against N, the average number of {110} interactions per stem, for calculation methods (a) (△) and (b) (×). Also plotted are the splittings for $(y\times2)$ groups (○) (from calculations in ref. 4). Individual groups are defined in brackets

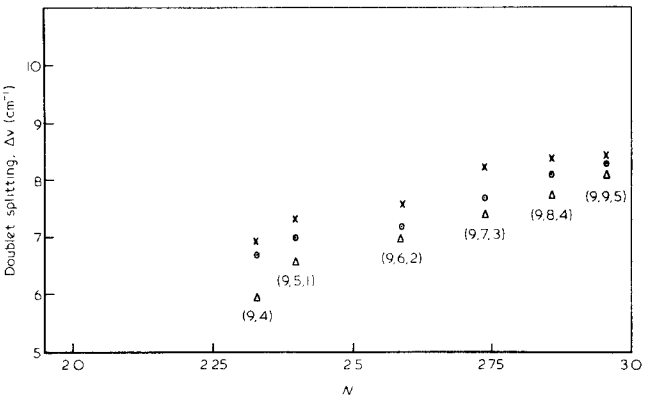

Figure 5 Calculated doublet splittings for (9, y, z) groups with $y=4,5, \ldots, 9$ and $z=y-4$. Values are plotted *versus* N for calculation methods (a) (△) and (b) (×). Also plotted in each case is the larger of $\Delta\nu_{(y\times2)}$ and $\Delta\nu_{(z\times3)}$(○) (from ref. 4). Individual groups are defined in brackets

The first bracketed expression in equation (2b) corresponds to the increase in splitting of group (y, y, z) over group $(z \times 3)$. The second such expression corresponds to the increase of (x, y, z) over that of (y, y, z). *Figure 5* shows the use of methods (a) and (b) for groups (9, 4), (9, 5, 1), (9, 6, 2), . . . , (9, 9, 5). Also shown is a splitting for a closed subgroup. As the number of sheets is >2, there is a choice of possible closed subgroups. Taking the group (9, 6, 2) as an example, there are two possibilities: (6×2) or (2×3). Clearly the larger of $\Delta\nu_{6\times2}$ and $\Delta\nu_{2\times3}$ will be closer to the true value of $\Delta\nu_{9,6,2}$. Calculations tabulated in ref. 4 show that $\Delta\nu_{6\times2}>\Delta\nu_{2\times3}$, and so $\Delta\nu_{6\times2}$ is plotted in *Figure 5* for the (9, 6, 2) group, alongside calculations using methods (a) and (b). Generally, the larger of $\Delta\nu_{y\times2}$ and $\Delta\nu_{z\times3}$ is used and denoted by $\Delta\nu_{\max}$. The inequality $\Delta\nu_{x,y,z}\geqslant\Delta\nu_{\max}$ is seen to apply for method (b), but not for method (a).

From this evidence, method (b) appears to give a better approximation to the splitting of an equivalent group of stems. The results can be compared with the direct calculations discussed previously: for the (3, 2) group, method (a) gives a value for $\Delta\nu_{3,2}$ of $5.17\ \text{cm}^{-1}$, method (b) $5.40\ \text{cm}^{-1}$ and the direct calculation $5.71\ \text{cm}^{-1}$. For the (5, 2) group the respective figures are 5.32, 5.80 and $5.84\ \text{cm}^{-1}$. In both cases method (b) gives a result in closer agreement with the direct calculation than method (a). The close agreement provides further justification for the general use of method (b).

It is now appropriate to summarize the procedure adopted for calculating splittings for different molecular models. Each molecular conformation generated by the computer model was first separated into independent groups of stems, which were in turn represented as equivalent groups. The splitting for each equivalent group was then calculated using equations (1b), (2b) etc. Some calculations were also made using method (a) and are discussed later.

EXPERIMENTAL RESULTS

Mixed crystals of PE were grown from dilute xylene solution at 70°C as described previously[6]. The preparation of dotriacontane ($C_{32}H_{66}$) mixed crystals has also been detailed elsewhere[8].

A Nicolet 7199 Fourier Transform Interferometer was used for i.r. measurements, with samples mounted in a cell

cooled to liquid nitrogen temperatures. A nominal resolution of 1 cm^{-1} was used, with approximately 500 scans for each spectrum. As individual band-widths are >1 cm^{-1}, as are the separations between components to be resolved, this resolution is adequate for the purposes here. (A resolution of 0.5 cm^{-1} was used for several spectra to verify this behaviour, and the results of curve fitting were only minimally affected). As discussed in earlier work, it became necessary at low PED concentrations to make allowance for a weak PEH absorption in the CD_2-bending region[8]. *Figure 6* shows the i.r. spectrum of PEH, crystallized at 70°C, in this region. The more intense sharp band at 1088 cm^{-1} falls in the middle of the CD_2-bending region, whereas the broader absorption centred at ≈ 1080 cm^{-1} is largely outside this region. The latter band formed the basis of the background subtraction procedure used: a PEH reference spectrum with a variable premultiplication factor was subtracted from each sample spectrum after conversion to linear absorbance, the premultiplier being adjusted until the 1080 cm^{-1} band disappeared. No estimate was made of the contribution to the CD_2-bending vibration from non-crystalline material.

Figure 7 shows the CD_2 bending region for samples with 0.5% PED for various molecular weights. In each case a PEH reference spectrum has been subtracted from the sample spectrum. The large improvement in signal-to-noise ratio compared with previous presults[8] reveals the general multiplet structure. The trend of increasing overall bandwidth with increasing molecular weight is confirmed. The separation between peaks at highest and lowest frequencies (the outermost doublet splitting corresponding to the outermost arrowed peaks) also clearly increases. The central minimum in absorbance becomes more pronounced with increasing molecular weight.

CALCULATIONS OF I.R. SPECTRA

As noted previously, the models derived from neutron scattering measurements involve the number of superfolded sheets increasing with molecular weight. Otherwise, all model parameters are kept independent of molecular weight. Molecular conformations (involving totals of up to 12 000 stems) were generated for various numbers of sheets. For each molecular conformation, a series of doublet splittings was calculated and the absorption intensities weighted as described previously.

The problem of summing the intensities from different doublets now arises. *Figure 8* shows the variation of peak frequency for fully deuterated dotriacontane (DD). The slopes of the two straight lines representing the high and low frequency components are $+5.3$ cm^{-1} and -3.5 cm^{-1}, respectively. (The central singlet is resolved only at low DD concentrations and shows no variation in frequency). The low frequency component is, therefore, less sensitive to the isotopic concentration than the high frequency component. For PE mixtures, varying the 'guest' molecular weight also has the effect of shifting the highest and lowest frequency components (see *Figure 7*). However, there is no indication of the lowest frequency components splitting into more than one band, and its frequency only changes by a small amount. As a first approximation, a common position for the low frequency component was, therefore, adopted. In addition, some allowance was made for natural and instrumental line-broadening. A Lorentzian lineshape was used, with a bandwidth equal to the experimental resolution (1.0 cm^{-1}). No singlet component was included in calcu-

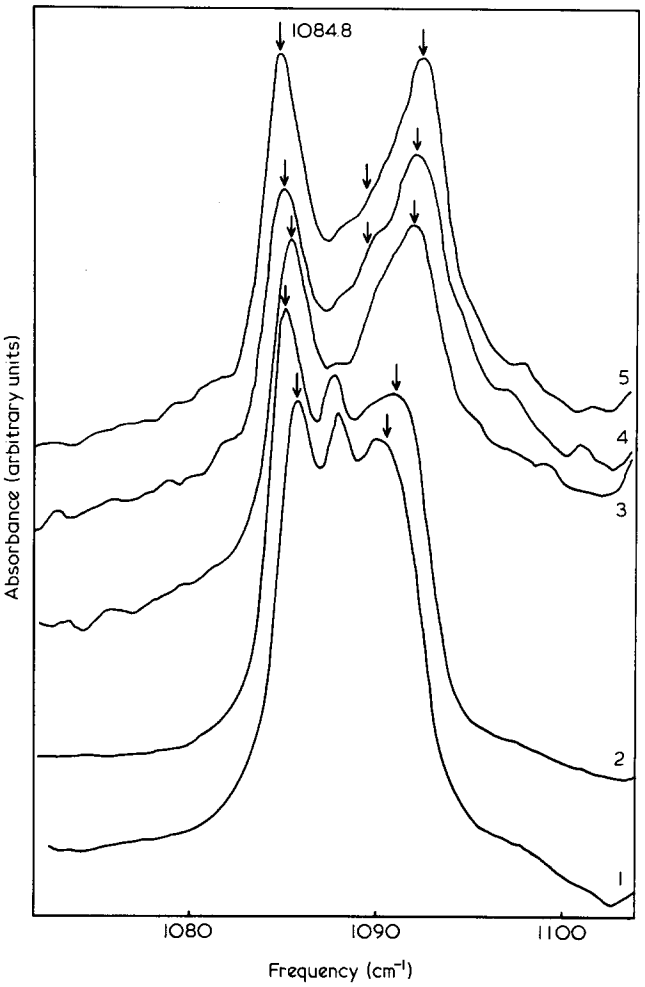

Figure 7 I.r. spectra for single crystal blends with 0.5% PED for molecular weights ($\bar{M}_w$) of 1, 46 000; 2, 69 000, 3, 155 000; 4, 216 000; 5, 386 000. In all cases a PEH reference spectrum, similar to that in *Figure 6*, has been subtracted. The position of doublet components obtained by curve fitting are arrowed

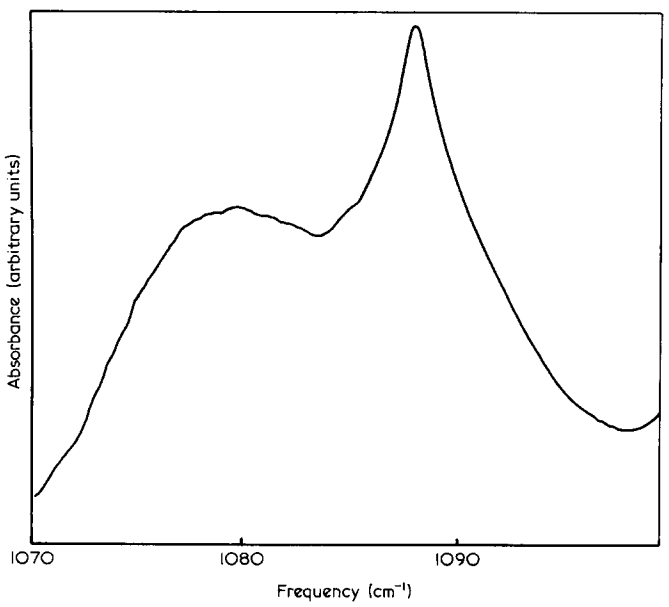

Figure 6 I.r. spectrum of a polyethylene single crystal mat

lations. This component arises from non-crystalline material, isolated crystal stems and rows of stems with fold directions other than {110}. The frequency appears to be sensitive to the fold arrangement[4] and uncertainties in the frequency position prevent any detailed analysis. It is emphasized that the use of a common low frequency component position is not expected to influence the qualitative conclusions on the *variation* of band profile with the number of sheets in the model.

Figure 9 shows calculations made in this way, and reproduces experimental peak widths to reasonable accuracy. Splittings corresponding to doublet peak separations in *Figure 9* are given in *Table 2*. As the number of sheets (N_{sh}) in the model system is increased, additional splittings appear, with the outermost splitting (components arrowed) progressively increasing. This is expected, as some progressively larger groups of stems are allowed with larger values of N_{sh}. The positions of lower frequency peaks change very little with N_{sh}, reflecting the fact that on increasing N_{sh} the types of smaller groups retained are similar. The relative intensities show marked changes, with the inner components losing intensity compared with the outermost doublet as N_{sh} increases. Clearly, the majority of stems are in the larger groups. This is illustrated by the maximum 7.0 cm^{-1} splitting into the 2 sheet model. As the number of sheets is increased to 4 and 11, the intensity of the highest frequency component increases with respect to the combined low frequency component, whilst progressively increasing in frequency. The absorption and profiles for 4 and 11 sheet models show marked similarities, with the outermost splittings (defined by the resolved peaks with highest and lowest frequencies (arrowed), the lowest frequency component being kept at constant frequency) differing by only 0.4 cm^{-1}. This reflects the similarity of the largest groups of stems in the two cases: the statistical arrangement of stems limits the number of sheets necessary in representing equivalent groups to a maximum of ≈ 4.

A comparison between the two methods of calculating doublet splittings is shown in *Figure 10*. In curve B the outermost doublet splitting is increased by 0.8 cm^{-1} and its high frequency component has a larger proportion of the total intensity. This supports the previous conclusions, i.e. that method (a) underestimates the magnitude of splittings for incomplete multiple sheets. However, the qualitative observations reported for the dependence of the i.r. spectrum on the number of sheets were found to be still valid for method (a).

Considering the absence of a central singlet in the curves of *Figure 9*, there are notable similarities between observed (*Figure 7*) and computed (*Figure 9*) spectra: the outermost doublet splitting increases with molecular weight, with the rate of increase decreasing rapidly for higher molecular weights. In both cases, the central minimum in absorbance becomes more pronounced as molecular weight increases.

It may seem surprising that a set of stem groups with different sizes and stem distributions should produce a series of discrete peaks in the calculated i.r. spectrum. The primary reasons for this are the large intervals between the doublet splittings of small groups (e.g.

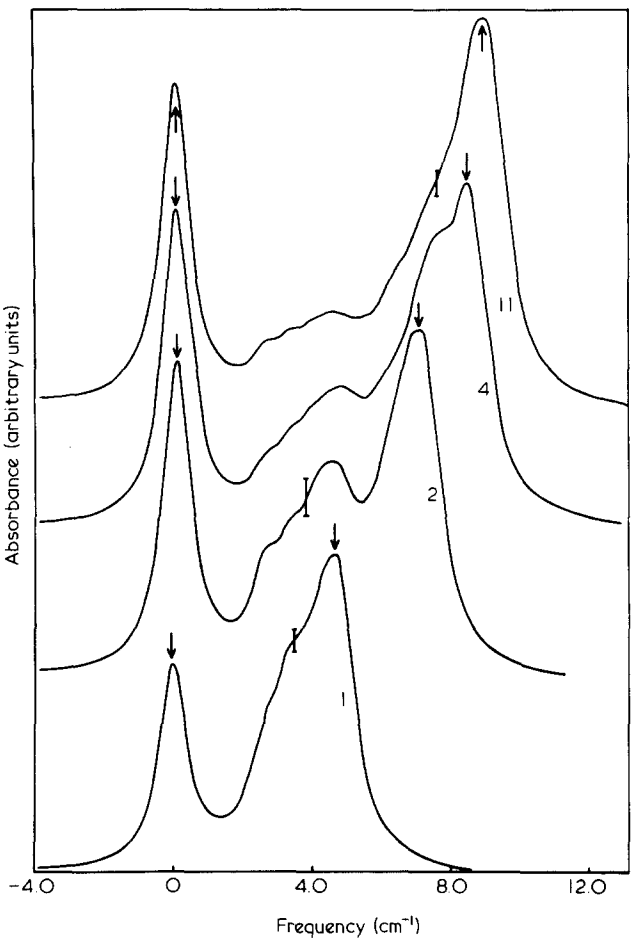

Figure 9 Computed i.r. spectra, using a Lorentzian broadening function of bandwidth 1 cm^{-1}. The frequency scale has been shifted so that the low frequency component corresponds to 0 cm^{-1}. Spectra are shown for 1, 2, 4 and 11 sheet models, with the same site occupation statistics as in *Figure 1*. A common low-frequency component has been used in each case, and reduced in intensity by comparison with the remainder of the profile by a factor of 3. Absorbance scales are the same except for the 1 sheet model, for which the scale is multiplied by 1.5. The ordinate scale is shifted for each model and the outermost doublet components are arrowed in each case. 1 sheet corresponds to an average molecular weight ($\bar{M}_w$) of 21 000. Error bars represent the maximum variation in intensity from different computer generations of stem arrangements

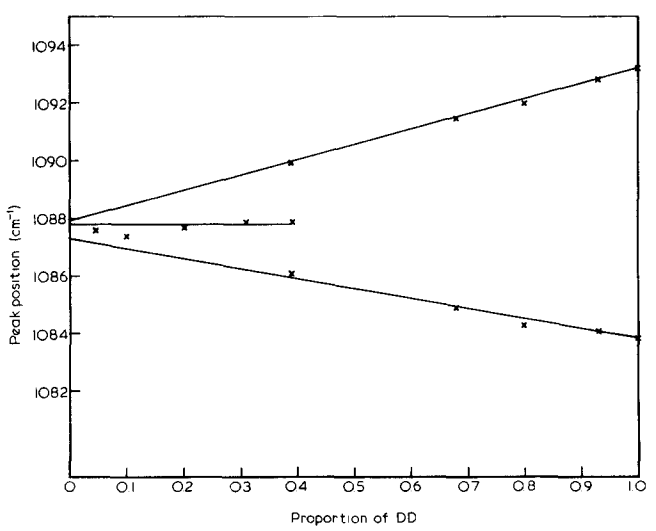

Figure 8 I.r. peak frequency positions for mixed crystals of dotriacontane mixtures *versus* concentration of d_{66}-dotriacontane (DD). The lines show the concentration dependence of high- and low-frequency components, and also the constant frequency of the central singlet which is resolved at lowest DD concentrations

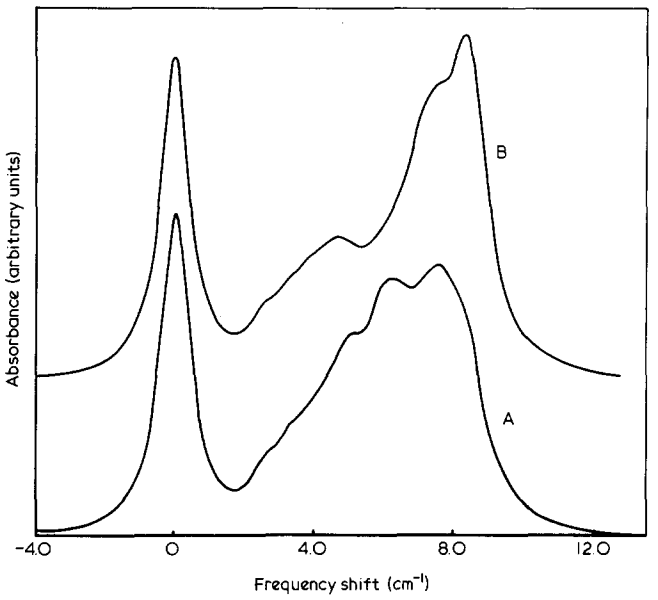

Figure 10 Computed i.r. spectra using the 4 sheet model, with a Lorentzian broadening function of bandwidth 1.0 cm^{-1}. The frequency scale has been shifted so that the low frequency component corresponds to 0 cm^{-1}. Curves A and B correspond to calculation methods (a) and (b). The scales are identical but the ordinate scale is shifted for the top curve

$(\Delta\nu_{3\times1}-\Delta\nu_{2\times1})$) and the large intervals between the asymptotic splittings for successively larger numbers of multiple sheets (e.g. $(\Delta\nu_{\infty\times2}-\Delta\nu_{\infty\times1})$). As discussed previously, the statistics of site occupancy determine the behaviour for large splittings.

Computer calculations based on the molecular models, therefore, show good agreement with experimental data, in particular reproducing the dependence of the band profile on molecular weight. The agreement of both neutron scattering and i.r. data with the molecular models used strengthens the evidence for a statistical preference for adjacent re-entry in solution-grown PE crystals: as indicated previously, the two techniques probe the molecular conformation over different scales. It is noted here that the i.r. technique has progressed from the stage where spectra were used to obtain simply a local concentration of guest stems[8]. The emphasis is now on the interactions of individual stems and the shape and size of groups to which they belong. Indeed, it is possible to construct models with the same dilution of labelled stems, but with different arrangements of stems, leading to quite different i.r. spectra. In particular a 'chequerboard' structure in which the local concentration was 50% but where no stems from the same molecule were adjacent along {110} would give *no* splitting. Similarly a preference for alternate lattice sites[9] would give very low splittings[12].

DECOMPOSITION OF MEASURED I.R. SPECTRA

The use of computer models to construct theoretical i.r. band profiles has been demonstrated in the previous section. An alternative approach, already noted, is the empirical decomposition of measured band profiles into an arbitrary number of component peaks. This method is used here for comparison with the computer modelling. While such a method leads to conclusions which are not fundamentally at variance with the analysis we have

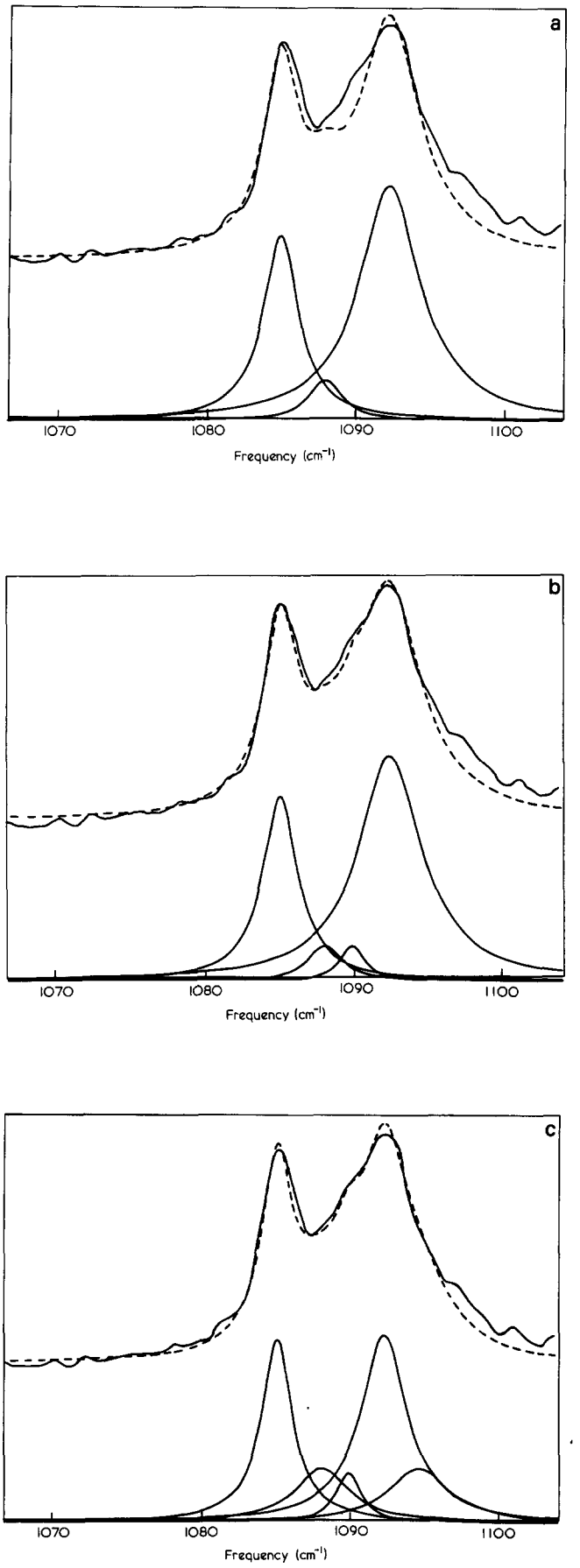

Figure 11 Examples of curve fitting on the i.r. data in fig. 7. (a), (b) and (c) show fits to one singlet and 1, 2 and 3 doublets. The fitted components are shown at the bottom and the sum of them is shown as a dashed line. Experimental data are from sample 4 ($\bar{M}_w$=216 000)

adopted, it will become clear that it has serious limitations, and is insensitive to the detailed arrangements of crystal stems.

The curve fitting (decomposition) used Lorentzian band profiles, with a common frequency for the low frequency component of each doublet (although the frequency *position* was allowed to vary between samples). As seen previously, *Figure 8* provides some justification for this assumption if PE single crystals behave in a similar way as a function of molecular weight (i.e. the low-frequency component varies less in frequency than the high-frequency component). From *Figure 7* the low-frequency component in mixtures with high PED molecular weight indeed appears narrower.

Results from curve fitting are shown in *Figure 11*. Parts (a), (b) and (c) represent fitting to a central singlet plus one, two and three doublets, respectively. The quality of fit is clearly poor in *Figure 11a* but improves for two doublets (*Figure 11b*). Further increasing the number of doublets continuously improves the fit. Peak positions corresponding to the fits in *Figure 11* are given in *Table 3*. The minimum number of doublets necessary to fit the data was, therefore, chosen to be 2. As in previous work[4], the general conclusion was that a minimum number of one doublet was necessary for low molecular weights and 2 for higher molecular weights. The results of this fitting procedure for all samples are given in *Table 4*, with doublet separations corresponding to separations between arrowed positions in *Figure 7*. It is noteworthy that the parameters obtained from the fitting are not unique: in particular, the component widths may be adjusted within relatively large limits without affecting the overall fit. The splittings in *Table 4* should, therefore, be seen as representative rather than unique. The profile of the singlet component, which can be seen from *Figures 11a—c* to change markedly with the type of fitting, has not been used in the analysis here. The proportion of absorption intensity within this singlet was found not to vary systematically with molecular weight. It is concluded that any analysis of the variation of singlet width with molecular weight should be treated with caution.

Table 3 Curve fitting on experimental data from sample 4

Frequency (cm^{-1})	Area (%)
A	
1092.3	65
1087.7	6
1085.1	29
B	
1092.3	63
1090.0	3
1087.7	5
1085.1	28
C	
1094.7	14
1092.3	42
1090.0	6
1087.7	12
1085.1	26

Returning to the details of *Table 4*, there is only a small variation in the smaller doublet splitting, but a progressive increase in the larger of the splittings with increasing molecular weight. For each sample, the arrangements of single and multiple sheets, whose calculated splittings correspond to the observed values, are given. Typical long spacings for PE single crystals grown at 70°C are of the order of 102 Å. Assuming a chain tilt of $\approx 30°$, the molecular weight per stem corresponds to ≈ 1300. Hence, in all cases, with one possible exception, an equivalent group does not correspond to a complete molecule. The possible exception is the higher splitting of 7.8 cm^{-1} in sample 5. Referring to *Table 2* of ref. 4, it is noteworthy that the doublet splitting for a double sheet of stems attains an asymptotic value of 7.7 cm^{-1} for a number of stems per sheet >16. The figure of 7.8 cm^{-1} quoted is, therefore, within 0.1 cm^{-1} of this asymptote. It then becomes impossible to define umambiguously a double sheet arrangement corresponding to the observed splitting, and the number of stems per sheet can only be specified as >16. Nevertheless, from *Table 4* the quoted block sizes correspond to progressively smaller fractions of the whole molecule as the molecular weight increases. It would seem unlikely that this general trend is not followed by sample 5, and it is believed that the 7.8 cm^{-1} splitting also corresponds to a small part of the whole molecule. The general pattern is in agreement with that for crystals grown at 85°C and on cooling to 55°C[4,5]. Cheam and Krimm have shown that the i.r. splittings for samples with $\bar{M}_w = 25\,900$ and 8700 are consistent with blocks of stems, each corresponding to most of a 'guest' molecule[4,5]. For higher molecular weights, the i.r. splittings were typical of blocks forming progressively smaller proportions of the complete molecule. The present work was restricted by sample availability to PED fractions with molecular weights ($\bar{M}_w$) $\geqslant 46\,000$, corresponding to the molecular weight range for which small angle neutron scattering is feasible. For lower molecular weights of 'guest' PED isotopic fractionation prevents measurements of the radius of gyration. Thus, there remains a range of molecular weight for which parallel neutron scattering and i.r. measurements are still not available.

Clearly, this simple curve fitting procedure verifies that groups of stems generally comprise only a small fraction of the whole molecule. However, by comparison with the results of calculations presented previously, this curve fitting leads to an interpretation of the molecular con-

Table 4 Results from the use of curve fitting on experimental infra-red data

Sample	$M_W \times 10^{-3}$	Doublet 1 splitting (cm^{-1})	Equivalent blocks of stems[a]	Doublet 2 splitting (cm^{-1})	Equivalent blocks of stems[a]
1	46	4.8	9 x 1	–	–
2	69	5.5	2 x 2; 3 x 2	–	–
3	155	4.6	7 x 1; 8 x 1	6.8	4 x 2
4	216	4.6	7 x 1; 8 x 1	7.2	6 x 8; 7 x 2
5	386	5.6	7 x 1; 8 x 1	7.8	3 x 3; >16 x 2

[a] Splittings for these blocks obtained from ref. 4.

formation which is a gross simplification and can only provide estimates of group dimemsions.

CONCLUSIONS

This good agreement between qualitative features of experimental and calculated i.r. spectra, together with the reasonable agreement for the magnitude of i.r. doublet splittings provides further support for the models for molecular conformation in solution-crystallized PE. Identical models have now been used to fit neutron scattering data over a wide angular range[1] and also to obtain good agreement with i.r. CD_2-bending vibration profiles for a range of molecular weights.

The favoured model (*Figure 1*) includes previously established features of superfolded sheets of stems, diluted by 0.5 along the fold plane. The detailed arrangement of chain stems (as originally derived from neutron scattering measurements[1]), involves $\approx 75\%$ adjacent re-entry and the statistics of site occupancy are independent of molecular weight. The arrangement of stems shown in projection at the top of *Figure 1* therefore, is, representative of all the sample molecular weights: only the number of superfolded sheets changes with molecular weight, with the molecular weight ($\bar{M}_w$) per sheet being 21 000. Evidence from previous i.r. work suggests that the statistics of site occupation change for molecular weights ($\bar{M}_w$) below the minimum value of 46 000[4,5] but this range of molecular weight was not investigated here because of the increased isotopic fractionation discussed previously.

ACKNOWLEDGEMENTS

Support for one of us (S.J.S.) from the SERC is acknowledged. The authors also thank Mrs A. Halter for technical assistance.

REFERENCES

1 Spells, S. J. and Sadler, D. M. *Polymer* 1984, **25**, 739
2 Tasumi, M. and Krimm, S. *J. Chem. Phys.* 1967, **46**, 755; and *J. Polym. Sci. A-2* 1968, **6**, 995
3 Bank, M. I. and Krimm, S. *J. Polym. Sci. A-2* 1969, **7**, 1785
4 Cheam, T. C. and Krimm, S. *J. Polym. Sci., Pol. Phys. Edn.* 1981, **19**, 423
5 Jing, X. and Krimm, S. *J. Polym. Sci. Pol. Phys. Edn.* 1982, **20**, 1155
6 Sadler, D. M., and Keller, A. *Macromolecules* 1977, **10**, 1128
7 Sadler, D. M. and Keller, A. *Science* 1979, **203**, 263
8 Spells, S. J., Sadler, D. M. and Keller, A. *Polymer* 1980, **21**, 1121
9 Yoon, D. Y. and Flory, P. J. *Disc. Faraday Soc.* 1979, **68**, 288
10 Lauritzen, J. I. and Hoffman, J. D. *J. Appl. Phys.* 1973, **44**, 4340
11 Zbinden, R. 'Infra-red Spectroscopy of High Polymers', Academic Press, New York, 1964, p 131 *et. seq.*
12 Spells, S. J. *Polymer* 1984 (*Commun.*) **24**, 162